How to reach a thousand-second in-plane polarization lifetime with 0.97-GeV/c deuterons in a storage ring

G. Guidoboni,[1] E. Stephenson,[2] S. Andrianov,[3] W. Augustyniak,[4] Z. Bagdasarian,[5,6] M. Bai,[6,7] M. Baylac,[8] W. Bernreuther,[9,7] S. Bertelli,[1] M. Berz,[10] J. Böker,[6] C. Böhme,[6] J. Bsaisou,[11,6] S. Chekmenev,[12] D. Chiladze,[5,6] G. Ciullo,[1] M. Contalbrigo,[1] J.-M. de Conto,[8] S. Dymov,[6,13] R. Engels,[6] F.M. Esser,[14] D. Eversmann,[12] O. Felden,[6] M. Gaisser,[15] R. Gebel,[6] H. Glückler,[14] F. Goldenbaum,[6] K. Grigoryev,[12] D. Grzonka,[6] T. Hahnraths,[6] D. Heberling,[16,7] V. Hejny,[6] N. Hempelmann,[12] J. Hetzel,[6] F. Hinder,[12,6] R. Hipple,[10] D. Hölscher,[16] A. Ivanov,[3] A. Kacharava,[6] V. Kamerdzhiev,[6] B. Kamys,[17] I. Keshelashvili,[6] A. Khoukaz,[18] I. Koop,[19] H.-J. Krause,[20] S. Krewald,[6] A. Kulikov,[13] A. Lehrach,[6,7] P. Lenisa,[1] N. Lomidze,[5] B. Lorentz,[6] P. Maanen,[12] G. Macharashvili,[5,13] A. Magiera,[17] R. Maier,[6,7] K. Makino,[10] B. Mariański,[4] D. Mchedlishvili,[5,6] Ulf-G. Meißner,[11,6,7,21,22] S. Mey,[12,6] W. Morse,[23] F. Müller,[6] A. Nass,[6] G. Natour,[14,7] N. Nikolaev,[24,25] M. Nioradze,[5] K. Nowakowski,[17] Y. Orlov,[26] A. Pesce,[1] D. Prasuhn,[6] J. Pretz,[12,7] F. Rathmann,[6] J. Ritman,[6,7] M. Rosenthal,[12,6] Z. Rudy,[17] A. Saleev,[27] T. Sefzick,[6] Y. Semertzidis,[15,28] Y. Senichev,[6] V. Shmakova,[13] A. Silenko,[29,30] M. Simon,[6] J. Slim,[16] H. Soltner,[14] A. Stahl,[12,7] R. Stassen,[6] M. Statera,[1] H. Stockhorst,[6] H. Straatmann,[14] H. Ströher,[6,7] M. Tabidze,[5] R. Talman,[26] P. Thörngren Engblom,[31,1] F. Trinkel,[12,6] A. Trzciński,[4] Yu. Uzikov,[13] Yu. Valdau,[21,32] E. Valetov,[10] A. Vassiliev,[32] C. Weidemann,[6] C. Wilkin,[33] A. Wrońska,[17] P. Wüstner,[14] M. Zakrzewska,[17] P. Zuprański,[4] and D. Zyuzin[6]

(JEDI collaboration)

[1] *University of Ferrara and INFN, 44100 Ferrara, Italy*
[2] *Indiana University Center for Spacetime Symmetries, Bloomington, Indiana 47405, USA*
[3] *Faculty of Applied Mathematics and Control Processes, St. Petersburg State University, 198504 Petersburg, Russia*
[4] *Department of Nuclear Physics, National Centre for Nuclear Research, 00681 Warsaw, Poland*
[5] *High Energy Physics Institute, Tbilisi State University, 0186 Tbilisi, Georgia*
[6] *Institut für Kernphysik, Forschungszentrum Jülich, 52425 Jülich, Germany*
[7] *JARA–FAME (Forces and Matter Experiments), Forschungszentrum Jülich and RWTH Aachen University, 52056 Aachen, Germany*
[8] *LPSC Université Grenoble-Alpes, CNRS/IN2P3, Grenoble, Cedex, France*
[9] *Institut für Theoretische Teilchenphysik und Kosmologie, RWTH Aachen University, 52056 Aachen, Germany*
[10] *Department of Physics and Astronomy, Michigan State University, East Lansing, Michigan 48824, USA*
[11] *Institute for Advanced Simulation, Forschungszentrum Jülich, 52425 Jülich, Germany*
[12] *III. Physikalisches Institut B, RWTH Aachen University, 52056 Aachen, Germany*
[13] *Laboratory of Nuclear Problems, Joint Institute for Nuclear Research, 141980 Dubna, Russia*
[14] *Zentralinstitut für Engineering, Elektronik und Analytik, Forschungszentrum Jülich, 52425 Jülich, Germany*
[15] *Center for Axion and Precision Physics Research, Institute for Basic Science, 291 Daehak-ro, Yuseong-gu, Daejeon 305-701, Republic of Korea*
[16] *Institut für Hochfrequenztechnik, RWTH Aachen University, 52056 Aachen, Germany*
[17] *Institute of Physics, Jagiellonian University, 30348 Cracow, Poland*
[18] *Institut für Kernphysik, Universität Münster, 48149 Münster, Germany*
[19] *Budker Institute of Nuclear Physics, 630090 Novosibirsk, Russia*
[20] *Peter Grünberg Institut, Forschungszentrum Jülich, 52425 Jülich, Germany*
[21] *Helmholtz-Institut für Strahlen- und Kernphysik, Universität Bonn, 53115 Bonn, Germany*
[22] *Bethe Center for Theoretical Physics, Universität Bonn, 53115 Bonn, Germany*
[23] *Brookhaven National Laboratory, Upton, NY 11973 USA*
[24] *L.D. Landau Institute for Theoretical Physics, 142432 Chernogolovka, Russia*
[25] *Moscow Institute of Physics and Technology, 141700 Dolgoprudny, Russia*
[26] *Cornell University, Ithaca, New York 14850, USA*
[27] *Samara State Aerospace University, Samara, 443086, Russia*
[28] *Department of Physics, KAIST, Daejeon 305-701, Republic of Korea*
[29] *Research Institute for Nuclear Problems, Belarusian State University, 220030 Minsk, Belarus*
[30] *Bogoliubov Laboratory of Theoretical Physics, Joint Institute for Nuclear Research, 141980 Dubna, Russia*
[31] *Department of Physics, KTH Royal Institute of Technology, SE-10691 Stockholm, Sweden*
[32] *Petersburg Nuclear Physics Institute, 188300 Gatchina, Russia*
[33] *Physics and Astronomy Department, UCL, London, WC1E 6BT, UK*

This letter describes the observation of a deuteron beam polarization lifetime near 1000 s in the horizontal plane of a magnetic storage ring (COSY). This long spin coherence time was maintained

through a combination of beam bunching, electron cooling, sextupole field corrections, and the suppression of collective effects through beam current limits. This record lifetime is required for a storage ring search for an intrinsic electric dipole moment on the deuteron at a statistical sensitivity level approaching 10^{-29} e·cm.

PACS numbers: 29.20.db, 29.27.Bd, 29.27.Hj, 29.85.Ca

This letter describes a significant advance in the ability to retain the usually short-lived horizontal (ring plane) part of the spin polarization of a deuteron beam ($p = 0.97$ GeV/c) using the COSY [1] magnetic storage ring. The preservation of this in-plane polarization (IPP) is a requirement for using a storage ring to search for an electric dipole moment (EDM) aligned along the spin axis of a subatomic system [2–5]. The COSY ring has a size comparable to that needed for such a search, polarized beams, polarimeters, and spin manipulation devices, making it an excellent place for such a demonstration.

In the EDM experiment, this IPP would be initially aligned with the deuteron momentum. The interaction between the EDM and the radial electric field always present in the storage ring particle frame [6–8] would cause the polarization to rotate about the radial direction, generating a vertical polarization component. This component would be observed at high sensitivity in a carbon target polarimeter [9]. The in-plane precession due to the anomalous part of the magnetic moment would be removed by choosing particular combinations of electric and magnetic bending fields for the storage ring. Feedback from the polarization measurements (to the beam revolution frequency) would be needed to keep the polarization direction longitudinal, parallel to the velocity. The requirement to have a long polarization lifetime on the order of 1000 s arises from the statistical sensitivity goal of 10^{-29} e·cm for the storage ring search (see Eq. (11.3) of [8]). At this level of precision, the observation of an EDM would demonstrate a hitherto unknown form of *CP* violation [2–4]. If only an upper limit is obtained, severe constraints would be provided on theories [10] of *CP*-violation that extend the Standard Model.

The goal of the COSY experiment was to demonstrate that a thousand-second IPP lifetime could be obtained in a magnetic storage ring without canceling the anomalous precession, thus using the IPP lifetime as a substitute for the "frozen spin" longitudinal component needed for EDM accumulation. In an ideal ring, the polarization component aligned along the ring's vertical magnetic field axis remains for a very long time and may be considered stable for our purposes. The IPP normally precesses around the vertical at the average rate of $\nu_S f_{\rm rev} = G\gamma f_{\rm rev} \sim 121$ kHz (G is the magnetic anomaly, γ is the relativistic factor, and $f_{\rm rev} = 750.603$ kHz is the beam revolution frequency). The IPP is subject to rapid depolarization (over tens of ms) due to small momentum variations (and hence γ variations) among the beam particles. This effect remains even if the anomalous rotation is cancelled. Standard tools for retaining the longitudinal polarization, such as the Siberian snake [11], are incompatible with EDM signal accumulation.

The recent implementation [12] of an event time-marking system at COSY has made it possible to unfold the in-plane precession and continuously measure the magnitude of the IPP. Considerable improvement in the IPP lifetime is obtained by bunching the beam with an rf cavity, ensuring isochronicity on average among the beam particles. Additionally, electron cooling [13] acts to reduce momentum spread, leading to polarization lifetimes of several seconds. Using the event time-marking system we can systematically adjust the sextupole fields and other properties in the ring with the aim of canceling second-order contributions to decoherence. The most important of these arises from small, transverse oscillations about the nominal orbit. In a bunched beam, such oscillations increase the path length around the ring, thereby increasing γ. Sextupole fields open the possibility to move the orbit for such oscillating particles to smaller radii in the storage ring arcs, thus compensating the path length increase. Previous work with electron rings [14] has found increased polarization lifetimes associated with small or zero chromaticities, a property also dependent on the sextupole fields. The chromaticities, ξ_x and ξ_y, are the derivatives of the betatron tunes, Q_x and Q_y, with respect to a change in the momentum, $\Delta p/p$, where the tunes are the number of oscillations the beam particles make in the transverse x and y directions in a single turn of the beam around the ring. In the electron ring experiments, an extension of a comparison of electron and positron magnetic moments [15, 16], adjustment of the sextupole fields yielded an IPP lifetime of about 0.8 s. It has been argued that the simultaneous appearance of zero chromaticity and long IPP lifetime should occur in general [17]. Shoji has explained the connection between increased pathlength and chromaticity [18]. At $Q_x \sim Q_y \sim 3.6$, the nearest spin resonances are too far away to matter [19]. Thus the zero chromaticity setting represents a starting point in the search for an optimal correction field. Lastly, it has been observed over the course of several experiments that operating with 10^9 deuterons/fill or less reduces beam instabilities (collective oscillations, beam blow-up) and problems with spurious polarization histories in the COSY ring.

Details of the experimental setup have been reported in Refs. [12, 20, 21]. The experiment made use of the EDDA scintillation detectors [22–24] as a polarimeter. The target was a 17-mm thick carbon block located 3 mm above

the beam centerline; vertical heating using electric field white noise brought beam particles to the target. The polarized beam, injected into COSY with the polarization axis vertical, had its axis rotated into the horizontal plane by the action of an rf-solenoid that operated on the $(1 - G\gamma)f_{\rm rev}$ spin resonance until the vertical polarization component vanished. Polarimeter events were tagged with a clock time that made it possible to assign an integer turn number from the beginning of the beam store. Multiplication of this number by ν_S, whose value was optimized in the analysis, yielded the total rotation angle of the IPP in revolutions. The fractional part of this angle gave the phase, which indicated the direction of the IPP in the ring plane. Once binned according to phase, the size of the IPP was obtained as the magnitude of a sine wave fit to the down-up counting rate asymmetries as a function of the phase angle. To record an IPP history, results were obtained for a series of short time intervals (typically 1 to 3 s) within the main beam storage time. Examples of these measurements are shown in Fig. 1 for two different values of the MXS and MXG sextupole strengths (both varied together). Three sextupole families, MXS, MXL, and MXG, are located in the COSY arcs at locations of large β_x, β_y, and dispersion (D) respectively. β_x and β_y are the Courant-Snyder parameters that describe the outer envelope of the beam; D is the correlation between the momentum deviation and the horizontal displacement of the particle track (see Chap. 2 of [25]). Measurements were made with two opposite polarization states injected on separate beam stores. This made possible systematic error checks associated with the vertical polarization component. Once rotated into the horizontal plane, both states yield an IPP with a positive magnitude. These were separately normalized to unity, then the data for the two states were averaged to produce the results shown in Fig. 1.

On the basis of an initial search within each time bin, a value of ν_S was found that gave the largest IPP. Then the average ν_S was obtained for each machine cycle. With this fixed, the unfolding analysis was repeated. This second sine wave fitting process determined for each time bin a phase for the down-up polarimeter asymmetries representing the polarization direction in the horizontal plane (see Fig. 2 of [26]). The phases were observed to vary smoothly with time (see Fig. 3a of [26]) and could be reproduced with a quadratic polynomial. Constraining both ν_S and the phase allowed the IPP to be determined without the positive bias present in a random distribution of asymmetries, as described in Ref. [12].

The time curves in Fig. 1 follow a shape that represents the polarization loss for a beam with equal horizontal and vertical emittance profiles after electron cooling. The calculated depolarization curves were based on a set of betatron amplitudes whose distribution was unfolded from measured beam profiles. The normalizations and the time scales for the curves in Fig. 1 were adjusted

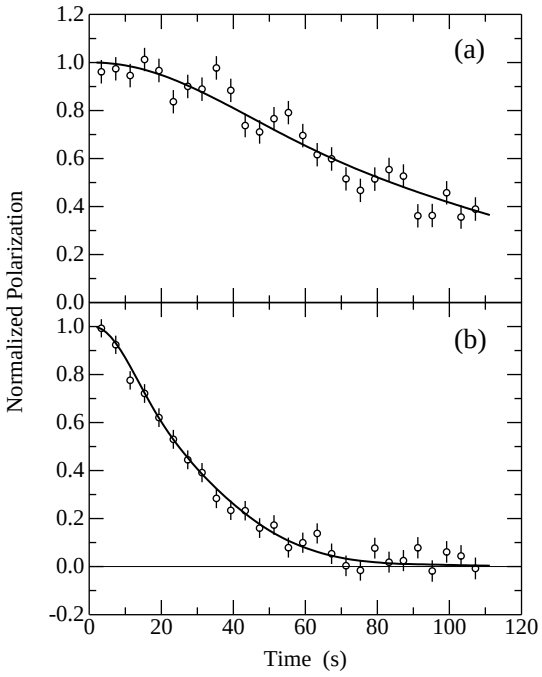

FIG. 1. Measurements of the IPP as a function of time after the polarization was rotated into the horizontal plane. The scale is set so that the normalized polarization is unity at $t = 0$ s. The measurements were made with two beam polarization states, separately normalized and then averaged. The two panels represent two different sextupole magnet settings, resulting in polarization lifetimes, defined as the time for the normalized IPP to reach 0.606, of 64.7 ± 5.4 s and 18.6 ± 2.6 s in panels (a) and (b) respectively.

to best reproduce the measurements. The IPP lifetime quoted is the time for the normalized polarization to fall to 0.606. In addition to the statistical error of the fitting process, the errors in the IPP lifetime include systematic contributions from errors in determining the initial polarization magnitude, the start time for the depolarization, and the construction of the polarization template curve shape.

In separate measurements, the chromaticities for a range of sextupole settings were obtained with a coasting beam by observing the shift of the x and y betatron tunes, Q_x and Q_y, taken from a frequency analysis of signals from beam pickups as the beam momentum was varied by changing the energy of the cooling electron beam. For an $B_{\rm MXL}$ setting of -0.29 m^{-3}, both chromaticities were found to be zero close to the line $B_{\rm MXS} = 6.0$ m^{-3} $- 3.1 \cdot B_{\rm MXG}$ connecting the magnet fields for these two sextupole families. The sextupole strength is given as the ratio of the second derivative of the vertical magnetic field with respect to the radial direction at $y = 0$ (in T/m^2) and the magnetic rigidity (in T·m). To emphasize variations in the polarization lifetime, the $B_{\rm MXS}$ and $B_{\rm MXG}$ magnet values were varied along a line perpendicular to this one. The data of Fig. 1 are representative of two

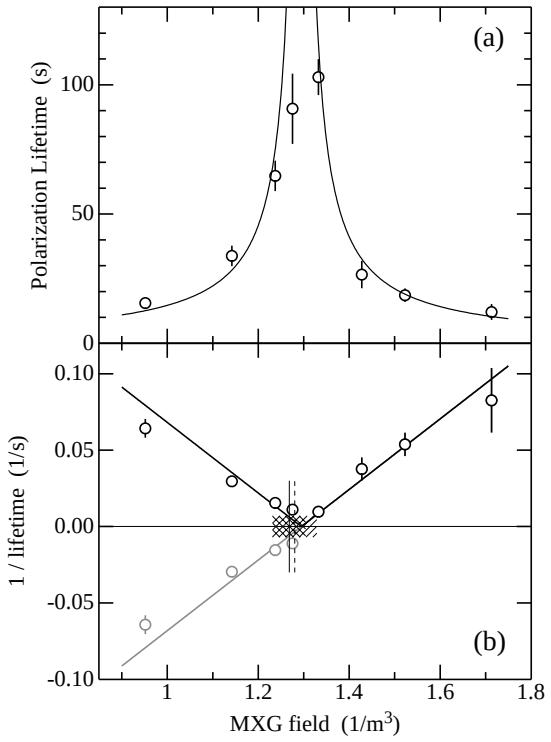

FIG. 2. (a) Values of the horizontal polarization lifetime as a function of the field in the MXG sextupole family (with MXS also varied). (b) The reciprocal of the lifetime values and their reproduction by Eq. (1). To make the linear result more obvious, all data points and the linear fit values at magnetic fields less than the zero chromaticity points (~ 1.3 m^{-3}) have been reversed in sign and replotted in gray. The lifetime curve in (a) is the reciprocal of the linear fit.

settings in this scan.

The top panel in Fig. 2 shows the lifetimes for 8 choices of sextupole strengths on either side of the zero chromaticity point (shown by the vertical solid (x) and dashed (y) lines in the lower panel with hash bands indicating the respective errors). The variation in lifetime is large, with a clear preference for the longest values near $B_{\rm MXG} = 1.3$ m^{-3}.

A preliminary investigation of the effects of the sextupole magnet families on the spread of ν_S values using the tracking program COSY INFINITY [27] showed a linear dependence of the reciprocal of the IPP lifetime on sextupole magnet currents, leading to the form

$$\frac{1}{\tau} = |A+a_S S+a_L L+a_G G|\theta_x^2+|B+b_S S+b_L L+b_G G|\theta_y^2 \ , \quad (1)$$

where θ_x^2 and θ_y^2 are the contributions of horizontal and vertical emittance, denoted by the square of the angle between the particle path and the reference orbit. τ is the IPP lifetime. S, L, and G are the sextupole magnet currents, with A and B representing the contributions to decoherence with no sextupole corrections. The a_i and b_i are coefficients for the sextupole currents determined by the emittance and dispersion at the location of the sextupole magnets. The B term also includes contributions from the so-called pitch effect [28] since these also depend on θ_y^2. A linear function serves to describe the measurements in the lower panel of Fig. 2. To illustrate that this is indeed the case, the measurements at $B_{\rm MXG} < 1.295$ m^{-3} were reversed in sign and shown as the gray points along with an extension of the straight line. The zero crossing point of the fit is close to the zero chromaticity point, fulfilling the expectation that long IPP lifetime and zero chromaticity occur together with the same sextupole magnet fields. The linear function in Fig. 2 arises if one of the two terms in Eq. (1) dominates and only one or a fixed combination of sextupole currents is varied. It is not a complete description of the IPP as a function of sextupole current, but does serve here to locate the sextupole current associated with the longest IPP.

A measured map of the chromaticites, ξ_x and ξ_y, showed that they varied linearly with the currents in the sextupole magnets. The slopes of the chromaticity with changing sextupole magnet current generally reproduce from one machine setup to another and agree with lattice models using COSY INFINITY. However, the zero offset, and hence the location of the zero values, varies considerably from one experimental setup to another, depending on the quality of orbit corrections, electron cooler steering, and other similar factors. For the COSY lattice, zero chromaticity for either x or y lies in a plane in MXS×MXL×MXG space. The intersection of these x and y zero planes is a line that is nearly constant in $B_{\rm MXL}$ ($= -0.14$ m^{-3}). Thus, a more thorough investigation is possible by exploring MXS×MXG space at a fixed value of MXL, which is shown in Fig. 3 along with the lines for zero x and y chromaticity (including their error bands).

In four different spots in Fig. 3 a short scan was made varying either MXS or MXG while holding the other and MXL constant. Polarization lifetime measurements similar to Fig. 1 were generated with a horizontally heated beam (to enhance sensitivity to sextupole changes) and analyzed as in Fig. 2 to locate the point of maximum lifetime. Those points are located in Fig. 3 using open circles (that are larger than the error in the location of the points). A second beam setup was used in which the cooling was completed first and then the coasting beam was bunched, which led to a longitudinally extended beam bunch. The measurements were repeated, yielding the crosses. The larger synchrotron oscillation amplitudes can create a larger $(\Delta p/p)^2$ spread in the beam that would add another major term to Eq. (1). But this effect seems to be smaller than the first two terms of which the vertical one is enlarged by vertical heating, so the new term does not appear in Eq. (1). As in the lower panel of Fig. 2, the maximal values of polarization lifetime are located at places that are consistent with zero x and y

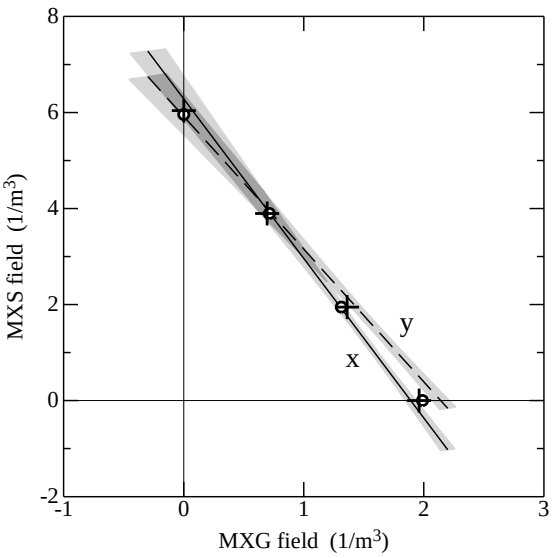

FIG. 3. This figure represents the MXS×MXG plane where $B_{\mathrm{MXL}} = -0.14$ m^{-3}. The gray bands represent the error about the lines of zero x and y chromaticity. Scans of MXS and MXG sextupole family currents found several local points of maximal IPP lifetime. The circles represent a beam setup with horizontal heating; the plus signs represent runs with enhanced longitudinal width. The error bars are smaller than the points.

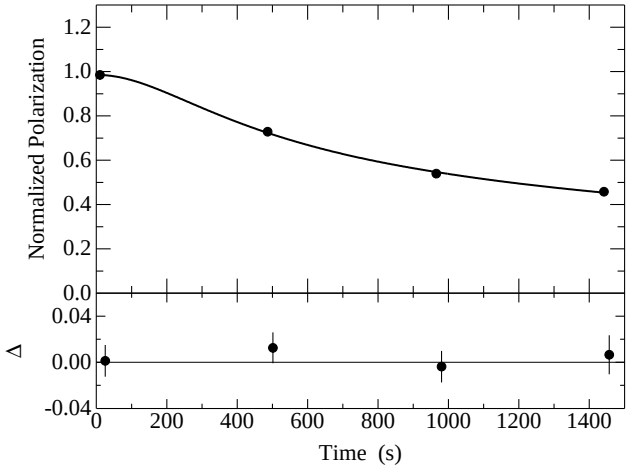

FIG. 4. Measurements of the normalized polarization. Least squares fits were made to the data acquired after rotation into the horizontal plane during four periods when the beam was extracted onto the polarimeter target. Data points taken with target extraction off are not shown. The residuals of the fit are given in the lower panel. The IPP lifetime is 782 ± 117 s.

chromaticity.

The largest values of the polarization lifetime in a more recent machine setup were found where $B_{\mathrm{MXS}} = 2.6$ m^{-3} and $B_{\mathrm{MXG}} = 1.2$ m^{-3}. A new machine setup with longer storage times was prepared with a lower beam current (about 10^9 deuterons/fill) and less collective motion to make ring operation more stable. Then this point in sextupole space was retested. Fig. 4 shows a measurement of the lifetime when the precooling of the beam lasted 75 s. To conserve beam, there were only four times when the vertical heating was on and the beam polarization sampled. The data were analyzed using a polynomial to reproduce the phase, as described for the measurements of Fig. 1. Each of the four sampling periods was treated separately. Within each period (about 15 s), the IPP measurements rose with time. The average of these points for each period is shown in the figure. The error includes the systematic effects of the uncertainty of the normalization of these data and a factor associated with the rising points in each extraction period. The error on each point is less than the size of the plotting symbol, so the residuals of the fit to the four data points are shown in a separate panel at the bottom of the figure.

An analysis with a template based on the unfolded distribution from beam profiles that was used for Fig. 1 fell too quickly with time and did not satisfactorily reproduce the time dependence of these data. Instead, a template [12] based on a Gaussian emittance distribution gave better agreement. The IPP lifetime is 782 ± 117 s. (The halflife of this template is 1173 ± 172 s. The time for this template to fall to 1/e of its original value is 2280 ± 336 s.)

Our experiments have demonstrated that it is possible to handle first-order (by bunching and electron cooling) and second-order (with sextupole fields) contributions to the polarization decoherence of a horizontally polarized beam in a magnetic storage ring. The improvement is three orders of magnitude in the horizontal polarization lifetime required for an EDM search using such a ring. The longest polarization lifetimes occur at sextupole magnet settings that are close to the places where the x and y chromaticites vanish, supporting a simple interpretation of the second-order decoherence in terms of the path lengthening associated with finite emittance. The present demonstration was built upon the earlier commissioning of continuous, high-efficiency polarization measurements coupled with a time-marking system that made the unfolding of the in-plane precession possible. The creation of a beam whose polarization always lies along the beam velocity is expected to be within reach using a suitable ring lattice and polarization measurements in a feedback loop system.

The authors wish to thank other members of the Storage Ring EDM Collaboration [29] for their help with this experiment. We also wish to acknowledge the staff of COSY for providing good working conditions and for their support of the technical aspects of this experiment. This work has been financially supported by the Forschungszentrum Jülich via COSY-FFE, the EU Integrated Infrastructure Initiative (FP7-10 INFRASTRUCTURES-2012-1, Grant Agreement No.

227431) and the Shota Rustaveli National Science Foundation of the Republic of Georgia. The work of UGM was also supported by the Chinese Academy of Sciences (CAS) President's International Fellowship Initiative (PIFI) (Grant No. 2015VMA076). This manuscript has been authorized by the Brookhaven Science Associates, LLC under Contract No. DE-SC0012709 with the US Department of Energy. This work was partially supported by IBS-R017-D1-2016-a00. G. Guidoboni acknowledges the support of a travel grant (FONDI 5 X 1000 ANNO 2011) from the University of Ferrara. N. Nikolaev and A. Saleev acknowledge support from the RScF Grant 16-12-10151.

[1] R. Maier, Nucl. Instrum. Methods Phys. Res. A **390**, 1 (1997).
[2] J. Engel, M. J. Ramsey-Musolf and U. Van Kolck, Prog. Nucl. Part. Phys. **71**, 75 (2013).
[3] W. Dekens, J. de Vries, J. Bsaisou, W. Bernreuther, C. Hanhart, Ulf-G. Meißner, A. Nogga, and A. Wirzba, J. High Energy Phys. **7**, 069 (2014).
[4] J. de Vries and Ulf-G. Meißner, arXiv:1509.07331.
[5] F.-K. Guo, R. Horsley, U.-G. Meißner, Y. Nakamura, H. Perlt, P.E.L. Rakow, G. Schierholz, A. Schiller, and J.M. Zanotti, Phys. Rev. Lett. **115**, 062001 (2015).
[6] F. J. M. Farley, K. Jungmann, J. P. Miller, W. M. Morse, Y. F. Orlov, B. L. Roberts, Y. K. Semertzidis, A. Silenko, and E. J. Stephenson, Phys. Rev. Lett. **93**, 052001 (2004).
[7] Y. F. Orlov, W. M. Morse and Y. K. Semertzidis, Phys. Rev. Lett. **96**, 214802 (2006).
[8] Proton EDM proposal found at `http://www.bnl.gov/edm`.
[9] N. P. M. Brantjes *et al.*, Nucl. Instrum. Methods Phys. Res. Sect. A **664**, 49 (2012).
[10] M. Pospelov and A. Ritz, Ann. Phys. **318**, 119 (2005).
[11] A. D. Krisch *et al.*, Phys. Rev. Lett. **63**, 1137 (1989).
[12] Z. Bagdasarian *et al.*, Phys. Rev. ST Accel. Beams **17**, 052903 (2014).
[13] H. Poth, Phys. Rep. **196**, 135 (1990).
[14] I. Vasserman *et al.*, Phys. Lett. B **198**, 302 (1987).
[15] S. Serednyakov, V.A. Sidorov, A.N. Skrinsky, G.M. Tumaikin, and Ju.M. Shatunov, Phys. Lett. B **66**, 102 (1977).
[16] I. Vassermann *et al.*, Phys. Lett. B **187**, 172 (1987).
[17] I.A. Koop and Ju.M. Shatunov, Proc. of the European Part. Accel. Conf. 1988 (Rome, Italy) p. 738.
[18] Y. Shoji, Phys. Rev. ST Accel. Beams **8**, 094001 (2005).
[19] M. Rosenthal, Ph.D. thesis, RWTH Aachen University, `http://collaborations.fz-juelich.de/ikp/jedi/`.
[20] P. Benati *et al.*, Phys. Rev. ST Accel. Beams **15**, 124202 (2012).
[21] P. Benati *et al.*, Phys. Rev. ST Accel. Beams **16**, 049901 (2013).
[22] E. Weise, Ph.D. thesis, Univ. of Bonn (2000), `http://edda.hiskp.uni-bonn.de/dipldiss.html`.
[23] D. Albers *et al.*, Eur. Phys. J. A **22**, 125 (2004).
[24] J. Bisplinghoff *et al.*, Nucl. Instrum. Methods Phys. Res. Sect. A **329**, 151 (1993).
[25] A. W. Chao, K. H. Mess, M. Tigner and F. Zimmermann, *Handbook of Accelerator Physics and Engineering* (World Scientific, 2012).
[26] D. Eversmann *et al.*, Phys. Rev. Lett. **115**, 094801 (2015).
[27] M. Berz and K. Makino, IOP J. Phys. **295**, 012143 (2011), `http://www.cosyinfinity.org`.
[28] F. J. M. Farley, Phys. Lett. B **42**, 66 (1972).
[29] `http://www.bnl.gov/edm/`.